

Magnetoplasma resonances in two-dimensional electron rings

C. Dahl* and J. P. Kotthaus

Sektion Physik, Universität München, Geschwister-Scholl-Platz 1, 80539 München, Germany

H. Nickel and W. Schlapp

Telekom Forschungs- und Technologiezentrum, Am Kavalleriesand 3, 64295 Darmstadt, Germany

(Received 31 August 1993)

Employing millimeter-wave spectroscopy, we have studied the magnetoplasma excitations of a two-dimensional electron gas confined in a ring geometry. The observed spectrum decomposes into several high- and two low-frequency branches. For large magnetic fields the latter are identified as edge magnetoplasmons localized at the inner and outer boundary of the rings. With decreasing magnetic field the inner edge mode exhibits a crossover from antidotlike to dotlike behavior. The resonances can also be analyzed in terms of plasmons in a strip with periodic boundary conditions.

The investigation of plasma excitations in bounded two-dimensional electron systems (2DES's) ranging from classical disks to strongly confined quantum dots which contain only a few electrons is an active field of current research. Such studies have mostly been restricted to the simple case of circular disks.¹⁻⁸ This geometry together with the approximation of an external parabolic confinement potential leads to frequencies of the allowed dipole excitations of the form¹

$$\omega_{\pm} = \pm\omega_c/2 + (\omega_c^2/4 + \omega_0^2)^{1/2}, \quad (1)$$

where $\omega_c = eB/m^*$ is the cyclotron frequency and ω_0 the plasma frequency of the confined system at zero magnetic field. For a classical disk approximated by a thin oblate spheroid with diameter d the latter is given by $\omega_0^2 = 3\pi n_s e^2 / 8\epsilon\epsilon_0 m^* d$, where n_s denotes the 2D electron density. In a magnetic field B applied perpendicularly to the 2D plane the plasma resonance splits into two branches with the upper branch approaching ω_c , whereas the lower mode eventually decreases in frequency as $1/B$. This mode is connected with the presence of the boundary of the system and has hence been termed edge magnetoplasmon (EMP). The magnetic-field dependence in Eq. (1) holds regardless of the system size which is a consequence of the assumption of a parabolic potential and reflects the generalized Kohn theorem.⁹ For nonparabolic potentials or in inhomogeneous fields higher-lying modes^{7,10} can be excited in addition to the fundamental resonance (1).

The set of plasma oscillations for geometries that deviate from the disk shape can be expected to be distinctly different. This is demonstrated in the present paper for a 2DES confined in a ring geometry. Such a system may alternatively be considered as a disk with a repulsive scatter, also known as an antidot,¹¹⁻¹⁶ at its center. The observed resonances indeed exhibit features of the spectra of both dot and antidot systems. Which description prevails depends on the aspect ratio of the ring and on the magnetic-field strength. Around zero magnetic field the resonances are reminiscent of the modes in simple circu-

lar disks. At larger B two modes with negative magnetic-field dispersion develop, which we interpret as edge magnetoplasmons at the inner and outer boundary. For a narrow ring, the resonances can also be described as 1D plasmons^{17,18} whose wave vector is determined by the mean perimeter of the ring. Some aspects of our experimental data are consistent with a recent theoretical treatment of plasma excitations in rings in the screened hydrodynamic approximation;¹⁹ discrepancies originate from the fact that we here study the unscreened case.

We have investigated two ring geometries with about the same outer diameter, $d \approx 50 \mu\text{m}$, but different aspect ratios. The inner diameters are $d_i = 12 \mu\text{m}$ ("broad rings") and $30 \mu\text{m}$ ("narrow rings"), respectively. The patterns are etched into a standard molecular-beam-epitaxy-grown δ -doped GaAs-Ga_xAl_{1-x}As heterostructure containing a 2D electron gas with density $n_s = 2.3 \times 10^{11} \text{ cm}^{-2}$ and dc mobility $\mu = 1.2 \times 10^6 \text{ cm}^2/\text{Vs}$ at $T = 4.2 \text{ K}$. The rings are arranged in a square lattice covering an area of several mm^2 in order to increase signal strength. The samples, which are mounted in a Q -band waveguide, are studied with microwave transmission spectroscopy at $T = 4.2 \text{ K}$. We measure the amplitude and relative phase of the transmitted signal as a function of the magnetic field at fixed frequencies between 28 and 480 GHz. In a more limited frequency range and with less resolution in amplitude and phase we are also able to perform frequency sweeps at fixed magnetic field.

The transmission amplitude for the broad rings is displayed in Fig. 1. Together with the simultaneously recorded phase these spectra reveal a complex set of resonances. Plotting the observed resonance frequencies against magnetic field [Fig. 2(a)] one can recognize several distinct modes, two of which are seen to split into "doublets" at finite magnetic field. We label these modes with $\omega_{n\pm}$, $n = 0, 1, 2, \dots$, where n is the number of nodes in the radial direction. The second, angular index " \pm " can in general assume the values $\pm m$, but is here found to be restricted to $m = \pm 1$, hence our abbreviated notation.

The other azimuthal modes, having zero dipole moment, are not excited in the uniform external high-frequency field of our experimental setup. From the circular symmetry it further follows¹⁹ that $\omega_{n+} = \omega_{n-}$ at $B = 0$.

Whereas the above symmetry considerations apply equally for simple circular disks, there are marked changes in the magnetoplasma spectrum induced by the ring geometry. The most prominent difference as compared to the resonances in a simple disk is the behavior of the upper branch of the lowest doublet, the ω_{0+} mode. Near $B = 0$ this branch exhibits a positive magnetodispersion as expected for the upper branch of a circular disk where it would approach cyclotron resonance with in-

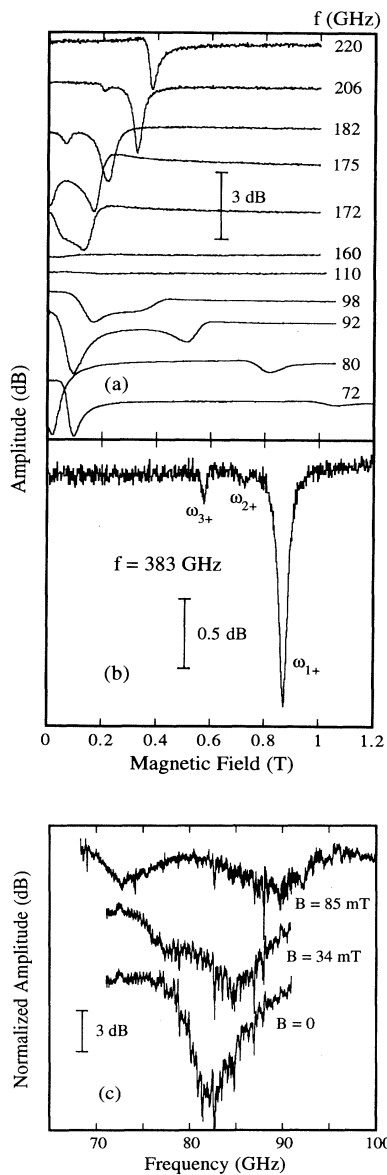


FIG. 1. Amplitude of the millimeter wave transmission for the array of electron rings with diameters $d = 50 \mu\text{m}$ and $d_i = 12 \mu\text{m}$, referred to as wide rings in the text. (a) and (b) show data at fixed frequency f vs magnetic field; (c) shows the normalized transmission vs frequency in the vicinity of zero magnetic field.

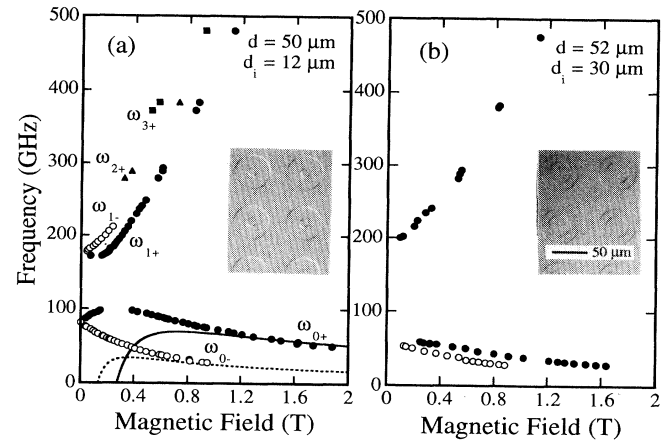


FIG. 2. Frequencies of the observed magnetoplasma resonances for two different ring geometries, (a) wide rings, (b) narrow rings (parameters are given in the text). In regions where the dispersion is flat the resonance positions cannot be resolved in our magnetic-field sweep experiments (ω_{0+} and ω_{1+} branches). The curves in (a) are dispersions calculated from Eq. (2) for $d = 12 \mu\text{m}$ (solid line) and $d = 50 \mu\text{m}$ (dashed line). The insets show micrographs of the corresponding sample surface.

creasing B . Here, however, above $B \approx 0.25$ T, the frequency of the ω_{0+} branch decreases with increasing magnetic field; at the same time its oscillator strength decreases rapidly. Both findings are known to be characteristic signatures of edge magnetoplasmons. These particular types of excitations have been shown to be localized at the edge of a 2DES at sufficiently large magnetic fields.^{20–23} They correspond to the ω_- mode of the simple parabolic model, Eq. (1). For larger B a better approximation for their dispersion for the case of a disk is²⁰

$$\omega_{\text{EMP}} = (\sigma_{xy} / \pi \epsilon \epsilon_0 d) [\ln(d/|l|) + 0.964], \quad (2)$$

where the modulus of $l = i\sigma_{xx} / \epsilon \epsilon_0 \omega$ is the length to which the EMP is localized at the edge and d is the disk diameter. Using the Drude model for the conductivity tensor and the appropriate sample parameters [$m^* = 0.068 m_e$, $\epsilon = (\epsilon_{\text{GaAs}} + 1)/2 = 6.8$, and $n_s = 2.3 \times 10^{11} \text{ cm}^{-2} / \text{Vs}$], Eq. (2) describes the data well for the ω_{0+} mode above $B \approx 1$ T without any adjustable parameters if d is set to the inner diameter of the ring as reflected in the solid line in Fig. 2(a). For the above reasons we are led to conclude that the high-field tail of the ω_{0+} mode constitutes an EMP localized at the inner boundary of the ring and thus may be called an antidot EMP. The lowest branch, the ω_{0-} mode, likewise exhibits a negative magnetodispersion together with a decreasing oscillator strength and is the EMP at the outer edge (the dot EMP). The above interpretation is substantiated by the observations in the narrow rings with the same outer, but larger inner diameter [Fig. 2(b)]. Here the frequency of the ω_{0+} mode has decreased whereas the frequency of the outer EMP remains almost unchanged (except near $B = 0$, where the modes are not localized). The ratio of the measured ω_{0+} frequencies for the two rings is precisely reproduced by Eq. (2) for magnetic fields above ≈ 1 T.

In a heuristic approach we determine the crossover field B_c , where the characteristics of the ω_{0+} mode change from bulk to edge behavior. Proceeding in the same spirit as above (i.e., approximating the antidot-EMP dispersion with the dot-EMP dispersion) and using Eq. (1) we find B_c from the condition that the frequency of the upper branch of a disk with the outer diameter be equal to the frequency of the lower branch of a disk with the diameter of the antidot, i.e., $\omega_+(d) = \omega_-(d_i)$. For the wide rings we thus obtain $B_c = 0.24$ T in good agreement with the observed transition field.

Turning to the higher-lying resonances, the “bulk magnetoplasmons” (BMP’s), we observe a marked splitting of the ω_1 mode. The oscillator strength of its upper branch rapidly decreases with increasing B , so that we observe it only up to ≈ 0.2 T. The lower branch of this doublet shows a negative magnetic-field dispersion at small B which can unambiguously be inferred from the polar plot (Fig. 3). In general, the splitting of all modes ω_n into doublets $\omega_{n\pm}$ is a consequence of the distinction between left- and right-handed electron motion in the presence of a magnetic field. For the EMP modes, the dot EMP (ω_{0-}) is connected with left-handed, the antidot EMP (ω_{0+}) with right-handed electron trajectories. To classify the BMP resonances ($n \geq 1$) we apply the theory of Ref. 19 and find that which branch of the BMP doublets is higher in energy depends on the aspect ratio d/d_i of the ring. For our structures with a comparatively low value ($d/d_i = 4.2$ for the wide rings) we obtain $\omega_{n-} > \omega_{n+}$,

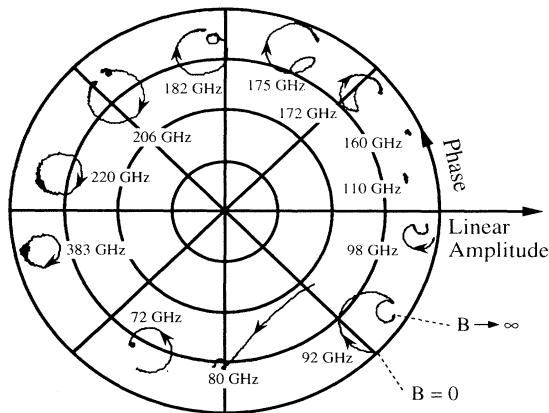


FIG. 3. Polar diagram (amplitude vs phase) corresponding to the amplitude data displayed in Figs. 1(a) and 1(b). Curve parameter is the magnetic field. Full coverage of a resonance in a sweep results in a closed circle. A partial sweep through a resonance leads to an arc segment. This is the case if a resonance is close to $B = 0$ or if a branch is not a monotonic function of B and is swept through twice. The sense of rotation along the curves with increasing magnetic field is clockwise (counterclockwise) for modes with positive (negative) magnetodispersion. In particular, the signals at 92, 98, and 172 GHz each exhibit one mode with positive and one with negative dispersion, whereas, e.g., for $f = 175$ GHz both of the two resonances belong to modes with positive dispersion.

which is the opposite of the situation in simple circular disks.^{7,23} It must, however, be kept in mind that, in contrast to the assumption made in Ref. 19, our rings are not screened by metallic electrodes. This leads to differences in the spectrum observed, in particular for the magnetic-field dispersion of the ω_{0+} branch which in the screened model is found to saturate at larger B always retaining a positive magnetodispersion. Nevertheless, the identification of the lower branch of the ω_1 mode as ω_{1+} is supported by the experimental observation that at larger B this branch contains almost all of the total oscillator strength. This is consistent with the fact that for large B the character of the dominant mode is cyclotron-resonance-like so that it is connected with right-handed electron trajectories. No doublets are observed for the highest, the ω_2 and ω_3 modes. Since these modes are weak [Fig. 1(b)] their upper branches ω_{2-} (ω_{3-}) presumably do not have sufficient strength to be resolved in our experimental setup, so that we only see the corresponding “+” branches. The total oscillator strength is primarily distributed among the ω_0 and ω_1 modes at small B and, as already mentioned, almost entirely contained in the ω_{1+} branch at larger magnetic field.

The ring spectrum displays marked analogies with the magnetoplasma resonances in antidot grids. Kern *et al.*¹² and Zhao *et al.*¹⁴ have observed two modes whose magnetic-field dependence is strongly reminiscent of the modes ω_{0+} and ω_{1+} . The analog of our ω_{0-} mode is absent in the antidot grid since that system has no outer boundary. Hence the lower mode of the antidot grid approaches cyclotron resonance as $B \rightarrow 0$ whereas in our finite system the ω_{0+} and ω_{0-} modes merge into a finite plasma frequency at zero magnetic field. Further, it is interesting to note that a mode corresponding to our ω_{1-} branch has recently been theoretically predicted for antidot grids,¹⁶ but has not been seen in the experiments.^{12,14} Our data reveal that such a resonance is likely to be a consequence of the ring geometry, i.e., the presence of an outer boundary of the system. Furthermore, in Ref. 16 the difference between the screened and unscreened limits for antidot grids has been explicitly worked out. The results suggest that an unscreened hydrodynamical calculation of electron rings would be able to reproduce our data.

Finally, we note that the excitations in the narrow rings [Fig. 2(b)] can also approximately be described as 1D magnetoplasmons with wave vector $q = 2/\bar{d}$, where \bar{d} is the mean diameter of the ring. From the calculations of Eliasson *et al.* (Fig. 2 in Ref. 18) we obtain $\omega_0 = 57$ GHz and $\omega_1 = 200$ GHz for our sample parameters for zero magnetic field, which is in good agreement with the experimental values extrapolated to $B = 0$. Within this model we can understand yet another experimental detail. For the wide rings the oscillator strength of the highest (ω_3) mode is larger than the strength of the ω_2 mode, which at first appears surprising as it is different for simple disks.²³ In a straight strip, however, only the modes with an odd number of nodes possess a finite dipole moment. Altering the symmetry of the strip by “bending” it to a ring leads to a nonzero moment also for the even modes yielding a small but discernible signal for

the ω_2 mode in the wide-ring geometry [Fig. 1(b)]. For the narrow rings the excitation of higher-order modes is obviously too weak to be observable for both even and odd modes.

In conclusion, the magnetoplasma excitations of the 2DES confined to a ring geometry exhibit intricate features which are determined by the interplay between geometrical parameters and the magnetic field. The spectrum decomposes into a set of high-frequency bulk magnetoplasma modes and two low-lying edge magnetoplasmons which can unambiguously be connected with the two boundaries of the ring. Since we have shown that the plasma resonances are to a great extent dominated by

geometric considerations, our results, although obtained for comparatively large structures, may serve as a guideline of what is to be expected for smaller, nanometer-scale systems, in particular for a quantum dot with a repulsive impurity at the center.

We thank M. Hartung, T. Heinzel, and A. Köck for valuable contributions and D. A. Wharam for a critical reading of the manuscript and acknowledge stimulating discussions with P. M. Petroff during the defining stages of this project. We gratefully acknowledge financial support from the Deutsche Forschungsgemeinschaft.

*Present address: France Telecom, CNET/PAB, 196 Avenue Henri Ravera, F-92220 Bagneux, France.

¹S. J. Allen, Jr., H. L. Störmer, and J. C. M. Hwang, *Phys. Rev. B* **28**, 4875 (1983).

²Ch. Sikorski and U. Merkt, *Phys. Rev. Lett.* **62**, 2164 (1989).

³T. Demel, D. Heitmann, P. Grambow, and K. Ploog, *Phys. Rev. Lett.* **64**, 788 (1990).

⁴A. Lorke, J. P. Kotthaus, and K. Ploog, *Phys. Rev. Lett.* **64**, 2559 (1990).

⁵F. Brinkop, C. Dahl, J. P. Kotthaus, G. Weimann, and W. Schlapp, in *High Magnetic Fields in Semiconductor Physics III*, edited by G. Landwehr (Springer, Heidelberg, 1992).

⁶D. B. Mast, A. J. Dahm, and A. L. Fetter, *Phys. Rev. Lett.* **54**, 1706 (1985).

⁷D. C. Glatzli, E. Y. Andrei, G. Deville, J. Poitrenaud, and F. I. B. Williams, *Phys. Rev. Lett.* **54**, 1710 (1985).

⁸A. L. Fetter, *Phys. Rev. B* **33**, 5221 (1985).

⁹L. Brey, N. F. Johnson, and B. I. Halperin, *Phys. Rev. B* **40**, 10 647 (1989).

¹⁰C. Dahl, J. P. Kotthaus, H. Nickel, and W. Schlapp, *Phys. Rev. B* **46**, 15 590 (1992).

¹¹K. Ensslin and P. M. Petroff, *Phys. Rev. B* **41**, 12 307 (1990).

¹²K. Kern, D. Heitmann, P. Grambow, Y. H. Zhang, and K. Ploog, *Phys. Rev. Lett.* **66**, 1618 (1991).

¹³A. Lorke, *Surf. Sci.* **263**, 307 (1991).

¹⁴Y. Zhao, D. C. Tsui, M. Santos, M. Shayegan, R. A. Ghanbari, D. A. Antoniadis, and H. I. Smith, *Appl. Phys. Lett.* **60**, 1510 (1992).

¹⁵V. Fessatidis, H. L. Cui, and O. Kühn, *Phys. Rev. B* **47**, 6598 (1993).

¹⁶G. Y. Wu and Y. Zhao, *Phys. Rev. Lett.* **71**, 2114 (1993).

¹⁷T. Demel, D. Heitmann, P. Grambow, and K. Ploog, *Phys. Rev. Lett.* **66**, 2657 (1991).

¹⁸G. Eliasson, J. W. Wu, P. Hawrylak, and J. J. Quinn, *Solid State Commun.* **60**, 41 (1986).

¹⁹C. R. Proetto, *Phys. Rev. B* **46**, 16 174 (1992).

²⁰V. A. Volkov and S. A. Mikhailov, *Zh. Eksp. Teor. Fiz.* **94**, 217 (1988) [*Sov. Phys. JETP* **67**, 1639 (1988)].

²¹I. Grodnensky, D. Heitmann, and K. v. Klitzing, *Phys. Rev. Lett.* **67**, 1019 (1991).

²²R. C. Ashoori, H. L. Störmer, L. N. Pfeiffer, K. W. Baldwin, and K. West, *Phys. Rev. B* **45**, 3894 (1992).

²³C. Dahl, in *Fortschritt-Berichte VDI*, Series 9 (VDI-Verlag, Düsseldorf, 1993), Vol. 165.

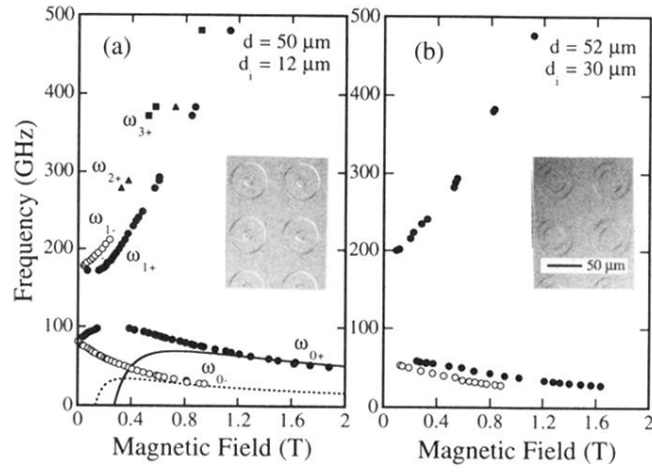


FIG. 2. Frequencies of the observed magnetoplasma resonances for two different ring geometries, (a) wide rings, (b) narrow rings (parameters are given in the text). In regions where the dispersion is flat the resonance positions cannot be resolved in our magnetic-field sweep experiments (ω_{0+} and ω_{1+} branches). The curves in (a) are dispersions calculated from Eq. (2) for $d = 12 \mu\text{m}$ (solid line) and $d = 50 \mu\text{m}$ (dashed line). The insets show micrographs of the corresponding sample surface.